Expansion of the Hadley cell under global warming: winter versus summer

Sarah M. Kang *

School of Urban and Environmental Engineering

Ulsan National Institute of Science and Technology, Ulsan, Republic of Korea

Jian Lu

Center for Ocean-Land-Atmosphere Studies, Institute of Global Environment and Society, Calverton, Maryland, and

Department of Atmospheric, Oceanic and Earth Sciences, George Mason University, Fairfax, Virginia

* *Corresponding author address:* Sarah M. Kang, School of Urban and Environmental Engineering, Ulsan National Institute of Science and Technology (UNIST), 100 Banyeon-ri, Eonyang-eup, Ulsan 689-798, Republic of Korea. E-mail: skang@unist.ac.kr

ABSTRACT

A scaling relationship is introduced to examine the seasonality in the outer boundary of the Hadley cell in both climatology and trend. In climatological state, the summer cell reaches higher latitudes than the winter cell since the Hadley cell in summer deviates more from the angular momentum conserving state, resulting in weaker upper-level zonal winds, which enables the Hadley cell to extend farther poleward before becoming baroclinically unstable. The Hadley cell can also reach farther poleward as the ITCZ gets farther away from the equator, hence more Hadley cell extension in solstices than equinoxes. In terms of trend, a robust poleward expansion of the Hadley cell is diagnosed in all seasons with global warming. The scaling analysis indicates this is mostly due to an increase in the subtropical static stability, which pushes poleward the baroclinically unstable zone and hence the poleward edge of the Hadley cell. The relation between the trends in the HC edge and the ITCZ is also discussed.

1. Introduction

The Hadley cell (HC), one of the most prominent circulation features on the face of the planet Earth, plays a pivotal role in shaping the tropical-to-subtropical climate. Its descending branch determines the location of the large-scale subtropical dry zone and its ascending branch determines the location of the inter-tropical convergence zone (ITCZ). The HC undergoes a continuous seasonal migration and is subject to the influence of the internal climate variability from interannual (Hou 1993, 1998; Chang 1995) to multi-decadal time scales (Mantsis and Clement 2009). In particular, the meridional extent of the HC is found to be responsive to climate change forcings such as greenhouse gas increase (Lu et al. 2007; Frierson et al. 2007) and stratospheric ozone depletion (Son et al. 2010; Kang et al. 2011).

Lu et al. (2007) found that CMIP3 models unanimously project a widening trend of the HC in their 21st century climate change scenarios and the subtropical dry zone expands poleward in accordance. They also tested two competing theories for the HC width: the nearly inviscid axisymmetric circulation theory (Schneider 1977; Held and Hou 1980) and the more heuristic view (Held 2000) that interprets the HC edge as being set by the criterion for baroclinic instability. By applying the two scaling theories to the annual-mean data, the HC expansion under global warming is found to be largely attributable to the increase of the subtropical static stability. Its stabilizing effect on the baroclinic waves at the poleward flank of the HC acts to extend the breakdown of the thermally direct angular momentum regime to a higher latitude.

However, since the annual-mean state is not physically realized in the real atmosphere,

it is questionable if the interpretation for the annual-mean change can be extended to each season given the nonlinear dynamics of the HC (Held and Hou 1980; Lindzen and Hou 1988; Plumb and Hou 1992; Fang and Tung 1999). For instance, the winter HC is relatively closer to the nearly inviscid limit while the summer HC is more subject to the influence of eddy momentum fluxes originated from the midlatitudes (Schneider and Bordoni 2008; Bordoni and Schneider 2009). To distinguish the contrasting dynamical regimes between the winter and summer cells, Walker and Schneider (2006) introduced a local Rossby number (Ro),

$$\mathrm{Ro} \equiv -\zeta/f \quad \text{where} \quad \zeta = -\frac{1}{a\cos\phi}\left(\frac{\partial}{\partial\phi}u\cos\phi\right) \text{ and } f = 2\Omega\sin\phi \tag{1}$$

where ζ is zonal-mean relative vorticity, f planetary vorticity, u the zonal-mean zonal wind, and Ω the Earth's angular velocity. Ro is a non-dimensional measure of the proximity of the tropical circulation to the inviscid angular momentum conserving (AMC) limit (Adam and Harnik 2012). It also measures the relative importance of the thermal driving versus the eddy driving for the mean meridional circulation. Hence, in the upper branches of the HC, Ro is large in the winter hemisphere and small in the summer hemisphere. We hereby develop a scaling theory that takes into consideration the different dynamical regimes undergone by the HC throughout the seasonal cycle by introducing the local Rossby number to the Held (2000) scaling, and this modified scaling theory is applied to each season.

We show that the application of the modified scaling to the cross-equatorial winter cell corroborates the interpretation of the Held (2000) for the annual-mean HC expansion under global warming, whereas it appears less adequate for the summer cell. Moreover, this exercise reveals an intriguing link between the locations of the ITCZ and the HC edge.

2. Scaling Theory

Following Held (2000), the HC edge can be viewed as the poleward limit of the angular momentum conservation (AMC) until the resulting vertical shear becomes baroclinically unstable. The scaling for the HC edge is obtained by solving the equations between the angular momentum conserving zonal wind and the baroclinically critical zonal wind. However, the angular momentum is not perfectly conserved especially in the upper branches of the summer HC. Hence, here we generalize the scaling to all seasons by dropping the constraint of AMC for the upper-level wind profile except between the ITCZ and the equator (Fig. 1). Instead, the local Rossby number, Ro in Eq. (1) is introduced that measures the extent to which the wind deviates from the AMC state. Ro is less than or equal to 1, with Ro=1 corresponding to the perfect AMC state.

Let's start with the cross-equatorial winter HC by integrating Eq. (1) from the equator to the winter HC edge, ϕ_w:

$$u_w \cos\phi_w - u_0 = \frac{\Omega a \mathrm{Ro}}{2}(1 - \cos 2\phi_w) \tag{2}$$

u_w denotes the zonal-mean zonal wind at $\phi = \phi_w$, and u at the equator, u_0, can be obtained as the zonal wind of an air parcel that would be attained under the assumption of AMC while moving to the equator from the ITCZ (ϕ_i), where it is at rest relative to the surface. This is a reasonable assumption since convective clouds in the ITCZ can effectively exchange momentum between the surface and the cloud top level. We then have $u_0 \approx -\Omega a \phi_i^2$, using small angel approximation, and substituting it into Eq. (2) gives:

$$u_w \approx \Omega a \mathrm{Ro} \phi_w^2 - \Omega a \phi_i^2. \tag{3}$$

Now, for the summer HC, we integrate Eq. (1) from the ITCZ to the summer HC edge, ϕ_s:

$$u_s \cos\phi_s = -\frac{\Omega a \mathrm{Ro}}{2}(\cos 2\phi_s - \cos 2\phi_i). \tag{4}$$

In the small angle approximation, Eq. (4) becomes

$$u_s \approx \Omega a \mathrm{Ro}\left(\phi_s^2 - \phi_i^2\right). \tag{5}$$

On the other hand, for the baroclinically unstable zonal wind velocity u_1, from the two-layer model's criterion for instability and thermal wind balance, we have

$$u_1 = \frac{g^*}{f}\frac{\partial H}{\partial y} = \beta\frac{g^* H_t}{f^2} \approx \frac{g^* H_t}{2\Omega a \phi^2} \tag{6}$$

where $g^* = g\Delta_v$ is the reduced gravity, with Δ_v the fractional change in potential temperature in the vertical, indicative of the tropospheric gross static stability. H_t is the mean thickness of the two-layer model, which is taken as the tropopause height. The HC edge can be obtained as the latitude at which the wind profiles Eqs. (3) or (5), depending on the season, coincides with Eq. (6). Eq. (3) is used when the ITCZ is located in the opposite hemisphere to the HC of interest, and Eq. (5) is used when the ITCZ is located in the same hemisphere as the HC.

To obtain the winter HC edge, we solve the equation $u_w = u_1$ or Eq. (3)=Eq. (6):

$$\phi_w^2 = \frac{\phi_i^2}{2\mathrm{Ro}} + \frac{1}{2\mathrm{Ro}}\left[\phi_i^4 + 2\mathrm{Ro}\left(\frac{g^* H_t}{\Omega^2 a^2}\right)\right]^{1/2}. \tag{7}$$

For the summer HC edge, we solve the equation $u_s = u_1$ or Eq. (5)=Eq. (6):

$$\phi_s^2 = \frac{\phi_i^2}{2} + \frac{1}{2}\left[\phi_i^4 + \left(\frac{2g^* H_t}{\Omega^2 a^2 \mathrm{Ro}}\right)\right]^{1/2}. \tag{8}$$

If ϕ_i=0 and Ro=1, then we retain the original Held's scaling: $\phi \propto \left(\frac{\Delta_v H}{\Omega^2 a^2}\right)^{1/4} \propto \left(\frac{NH}{\Omega a}\right)^{1/2}$, where N is the vertically averaged Brunt-Väisälä frequency, as in Lu et al. (2007).

3. Data and Methods

The model data retrieved from the AR4 archive is analyzed for 4 scenarios (1pctto2x; 20 models, 1pctto4x; 12 models, A1B; 22 models, and A2; 15 models) in DJF and JJA. Only the first ensemble member of each model is used. To identify the climate change response, we compute the linear trend for the 100-year period.

The HC edge, denoted as $\phi_{\Psi 500}$, is defined by the latitude of the first zero crossing–going poleward from the extremum–of the zonal-mean mass streamfunction Ψ at 500 hPa, computed by vertically integrating the zonal-mean density-weighted meridional wind component from the model top downward. The actual HC edge, $\phi_{\Psi 500}$ is compared with the scaled HC edge from Eq. (7) or (8) depending on the season.

We now describe how the variables in the scaling are computed. The ITCZ, ϕ_i is determined as the latitude of the zero crossing–in between the two extremum–of Ψ at 500 hPa. The tropopause height, H_t is computed from temperature data as the lowest pressure level at which the lapse rate decreases to 2°C/km, following the algorithm of Reichler et al. (2003). The static stability, Δ_v is computed as $\left(\theta(H_t) - \theta(1000hPa)\right)/(2\theta_m)$ where θ_m is the mean tropospheric potential temperature, set to be 290 K. In the scaling, we use the averaged $\Delta_v H_t$ between 20°S/N and 40°S/N. The local Rossby number, Ro is a free parameter to best match the scaled $\phi_{\Psi 500}$ with the actual $\phi_{\Psi 500}$ for the first 20 year mean. Ro varies with the hemisphere and season, but is kept unchanged with year and scenario: from DJF, MAM, JJA, to SON, the northern Ro=1.00, 0.95, 0.50, and 0.50, and the southern Ro=0.45, 0.50, 0.98, and 0.70. When the ITCZ is in the opposite hemisphere to the HC (DJF and MAM in the NH and JJA and SON in the SH), there is a strong cross-equatorial HC with Ro→1.

In contrast, when the ITCZ is in the same hemisphere as the HC (in the other two seasons), Ro is relatively small indicating the strong influence of eddy momentum fluxes.

4. Results

We first examine the extent to which the scaling relation works in predicting the seasonality in the *climatological mean* HC edge. Fig. 2 compares the first 20 year mean of the actual $\phi_{\Psi 500}$ in the abscissa with the scaled $\phi_{\Psi 500}$ in the ordinate for each season in both hemispheres. The seasonality in the mean HC edge is well captured by the scaling with an exception in the boreal summer cell: in general, the summer cell extends more poleward than the winter cell. In the NH JJA, the scaled $\phi_{\Psi 500}$ is larger than the actual $\phi_{\Psi 500}$ by 4° in the ensemble mean. The scaling relation is expected to not work well in boreal summer because the HC is very weak that the edge is ill-defined and that the cell is greatly affected by extratropical processes. The $\phi_{\Psi 500}$ seasonality can be mostly attributed to the seasonality in the value of Ro prescribed in the scaling, which is larger in winter and smaller in summer, since the scaled $\phi_{\Psi 500}$ is inversely proportional to Ro following Eqs. (7) and (8). A smaller Ro in summer indicates larger deviation from the angular momentum conserving wind u_{AMC} (Fig. 1), so that the weak summer HC can reach farther poleward until it becomes baroclinically unstable. Hence, as shown in Fig. 3, when the ITCZ is located in the same hemisphere (DJF and MAM for the SH, and JJA and SON for the NH), the HC edge reaches farther poleward than the other two seasons. In addition, for a given Ro, the absolute magnitude of the ITCZ latitude can contribute to the seasonality in the mean HC extent. This is implied in our scaling relation, Eqs. (7) and (8), which suggests that the HC extent for a fixed Ro is

proportional to the absolute magnitude of the ITCZ latitude. This is because in case of the ITCZ closer to the equator, u_{AMC} becomes baroclinically unstable faster (Fig. 1), resulting in a more equatorward HC edge. For example, despite similar magnitude of the prescribed Ro in DJF and MAM in both hemispheres, as the ITCZ is farther away from the equator in DJF, $\phi_{\Psi 500}$ in DJF is in the poleward side of the $\phi_{\Psi 500}$ in MAM. This seems to apply to the inter-model spread as well.

We next move on to the seasonality in the *trend* of the HC edge. As shown in Fig. 4, in terms of ensemble-mean, the HC edge extends more poleward in all scenarios and seasons, which is diagnosable by our scaling, with a couple of exceptions in boreal summer. This is again because the boreal summer cell is not a well defined zonal-mean feature. Considering that our scaling ignores the extratropical sources of change that are shown by a number of recent studies to affect the HC edge trend such as the rise of tropopause (Lorenz and DeWeaver 2007), increase of midlatitude eddy phase speed (Chen et al. 2008; Lu et al. 2008), upper level midlatitude baroclinicity (Rivi$\tilde{\text{e}}$re 2011), and the increase of the spatial scale of the midlatitude eddies (Kidston et al. 2010), the scaling works reasonably well in capturing the ensemble-mean trend of the HC edge, particularly in the SH. Thus, we proceed to examine what factors are responsible for the $\phi_{\Psi 500}$ trend based on the scaling relation with the focus on the SH.

Fig. 5 compares the actual $\phi_{\Psi 500}$ trend with its scaling for each model and scenario in austral winter and summer. Because the summer cell is more susceptible to the influence of the midlatitude eddies, the scaling is expected to work better in winter. Indeed, the correlation coefficient between the actual $\phi_{\Psi 500}$ trend and its scaling is higher in JJA (0.53) than in DJF (0.37). As the scaling works modestly in both seasons, we partition the trend

into changes in Δ_v and H_t, and changes in ITCZ location. A comparison between the middle and right panels indicates that the poleward shift is mostly due to changes in subtropical-to-midlatitude static stability and the associated tropopause rise, while the contribution of the ITCZ in the inter-model spread of the HC expansion is also discernible. The effect of the ITCZ trend on the $\phi_{\Psi 500}$ trend is illustrated in Fig. 6. The $\phi_{\Psi 500}$ trend in summer is positively correlated with the ITCZ shift and vice versa in winter. In austral winter (summer), the ITCZ is in the NH (SH), so that the positive ITCZ trend indicates a poleward (equatorward) shift. Hence, Fig. 6 indicates that $\phi_{\Psi 500}$ in both seasons shifts more equatorward as the ITCZ shifts more equatorward with climate change, a behavior consistent with the scaling relations Eqs. (7) and (8). This is consistent with what scaling suggests as in the climatological mean (Fig. 3) when Ro is kept similar. The opposite direction of movement between the winter HC edge and the ITCZ can be thought of as the result of the enhancement of the winter cell wind and its inclination towards instability as the ITCZ in the summer hemisphere moves equatorward (c.f. Fig. 1).

5. Summary and Discussion

We introduce a scaling theory for the HC edge that distinguishes contrasting dynamical regimes between the winter and summer cells by means of local Rossby number, Ro, following Walker and Schneider (2006). The HC edge is then determined as the poleward extent to which the zonal wind profile obtained from Ro continues until the resulting vertical shear becomes baroclinically unstable (Held 2000). As a follow-up study of Lu et al. (2007), we examine the seasonality of the scaling relationships by relaxing the assumption of AMC.

This scaling relation works well in explaining the seasonality in the climatological HC that the summer cell extends more poleward than the winter cell. This is primarily because of seasonality in the prescribed Ro, whose value is small in summer (indicative of great influence of extratropical eddies) and large in winter (indicative of being close to the AMC state). With smaller (larger) Ro, the zonal wind deviates more (less) from AMC wind profile, becoming much weaker (stronger) to be able to extend further (less) poleward before it becomes baroclinically unstable. Also, the HC edge extends more poleward in solstices than equinoxes because the ITCZ is located farther away from the equator, which delays the breakdown of the thermally driven cell to higher latitudes.

Furthermore, in both austral winter and summer, a robust poleward expansion of the HC in several scenarios of the 21st century with varying extent of CO_2 concentration increase is successfully diagnosed by our scaling relation. It suggests that the HC expansion in both seasons results from the increase in gross static stability and the tropopause rise near the subtropics, as in Lu et al. (2007) where only annual means have been analyzed. Also, the HC edge trend is shown to be related with the ITCZ trend: a larger HC expanding trend as the ITCZ gets farther away from the equator. Considering that the ITCZ responses with CO_2 increase are largely driven from the extratropics (Frierson and Hwang 2012), the extratropical dynamics seem to play a key role in the HC expansion with global warming.

Acknowledgments.

REFERENCES

Adam, O. and N. Harnik, 2012: Idealized annually averaged Macroturbulent Hadley Circulation in a Shallow Water Model, in preparation for. *J. Atmos. Sci.*

Bordoni, S. and T. Schneider, 2009: Regime Transitions of Steady and Time-Dependent Hadley Circulations: Comparison of Axisymmetric and Eddy-Permitting Simulations. *J. Atmos. Sci.*, **67 (5)**, 1643–1654.

Chang, E. K. M., 1995: The Influence of Hadley Circulation Intensity Changes on Extratropical Climate in an Idealized Model. *J. Atmos. Sci.*, **52 (11)**, 2006–2024.

Chen, G., J. Lu, and D. M. W. Frierson, 2008: Phase Speed Spectra and the Latitude of Surface Westerlies: Interannual Variability and Global Warming Trend. *J. Climate*, **21 (22)**, 5942–5959.

Fang, M. and K. K. Tung, 1999: Time-Dependent Nonlinear Hadley Circulation. *J. Atmos. Sci.*, **56 (12)**, 1797–1807.

Frierson, D. M. W. and Y.-T. Hwang, 2012: Extratropical Influence on ITCZ Shifts in Slab Ocean Simulations of Global Warming. *J. Climate*, **25 (2)**, 720–733.

Frierson, D. M. W., J. Lu, and G. Chen, 2007: Width of the Hadley cell in simple and comprehensive general circulation models. *Geophys. Res. Lett.*, **34 (18)**, L18 804, doi: 10.1029/2007GL031115.

Held, I. M., 2000: The general circulation of the atmosphere, paper presented at 2000 Woods Hole Oceanographic Institute Geophysical Fluid Dynamics Program, Woods Hole Oceanogr. Inst., Woods Hole, Mass. (Available at http://gfd.whoi.edu/proceedings/2000/PDFvol2000.html).

Held, I. M. and A. Y. Hou, 1980: Nonlinear Axially Symmetric Circulations in a Nearly Inviscid Atmosphere. *J. Atmos. Sci.*, **37 (3)**, 515–533.

Hou, A. Y., 1993: The Influence of Tropical heating Displacements on the Extratropical Climate. *J. Atmos. Sci.*, **50 (21)**, 3553–3570.

Hou, A. Y., 1998: Hadley Circulation as a Modulator of the Extratropical Climate. *J. Atmos. Sci.*, **55 (14)**, 2437–2457.

Kang, S. M., L. M. Polvani, J. C. Fyfe, and M. Sigmond, 2011: Impact of Polar Ozone Depletion on Subtropical Precipitation. *Science*, **332 (6032)**, 951–954.

Kidston, J., G. K. Vallis, S. M. Dean, and J. A. Renwick, 2010: Can the Increase in the Eddy Length Scale under Global Warming Cause the Poleward Shift of the Jet Streams? *J. Climate*, **24 (14)**, 3764–3780.

Lindzen, R. S. and A. V. Hou, 1988: Hadley Circulations for Zonally Averaged Heating Centered off the Equator. *J. Atmos. Sci.*, **45 (17)**, 2416–2427.

Lorenz, D. J. and E. T. DeWeaver, 2007: Tropopause height and zonal wind response to global warming in the IPCC scenario integrations. *J. Geophys. Res.*, **112 (D10)**, D10 119, doi:10.1029/2006JD008087.

Lu, J., G. Chen, and D. M. W. Frierson, 2008: Response of the Zonal Mean Atmospheric Circulation to El Niño versus Global Warming. *J. Climate*, **21 (22)**, 5835–5851.

Lu, J., G. A. Vecchi, and T. Reichler, 2007: Expansion of the hadley cell under global warming. *Geophys. Res. Lett.*, **34 (6)**, L06 805, doi:10.1029/2006GL028443.

Mantsis, D. F. and A. C. Clement, 2009: Simulated variability in the mean atmospheric meridional circulation over the 20th century. *Geophys. Res. Lett.*, **36 (6)**, L06 704, doi: 10.1029/2008GL036741.

Plumb, R. A. and A. Y. Hou, 1992: The Response of a Zonally Symmetric Atmosphere to Subtropical Thermal Forcing: Threshold Behavior. *J. Atmos. Sci.*, **49 (19)**, 1790–1799.

Reichler, T., M. Dameris, and R. Sausen, 2003: Determining the tropopause height from gridded data. *Geophys. Res. Lett.*, **30 (20)**, 2042, doi:10.1029/2003GL018240.

Rivière, G., 2011: A Dynamical Interpretation of the Poleward Shift of the Jet Streams in Global Warming Scenarios. *J. Atmos. Sci.*, **68 (6)**, 1253–1272.

Schneider, E. K., 1977: Axially Symmetric Steady-State Models of the Basic State for Instability and Climate Studies. Part II. Nonlinear Calculations. *J. Atmos. Sci.*, **34 (2)**, 280–296.

Schneider, T. and S. Bordoni, 2008: Eddy-Mediated Regime Transitions in the Seasonal Cycle of a Hadley Circulation and Implications for Monsoon Dynamics. *J. Atmos. Sci.*, **65 (3)**, 915–934.

Son, S.-W., et al., 2010: Impact of stratospheric ozone on southern hemisphere circulation change: A multimodel assessment. *J. Geophys. Res.*, **115**, D00M07, doi:10.1029/2010JD014271.

Walker, C. C. and T. Schneider, 2006: Eddy influences on hadley circulations: Simulations with an idealized gcm. *J. Atmos. Sci.*, **63 (12)**, 3333–3350.

List of Figures

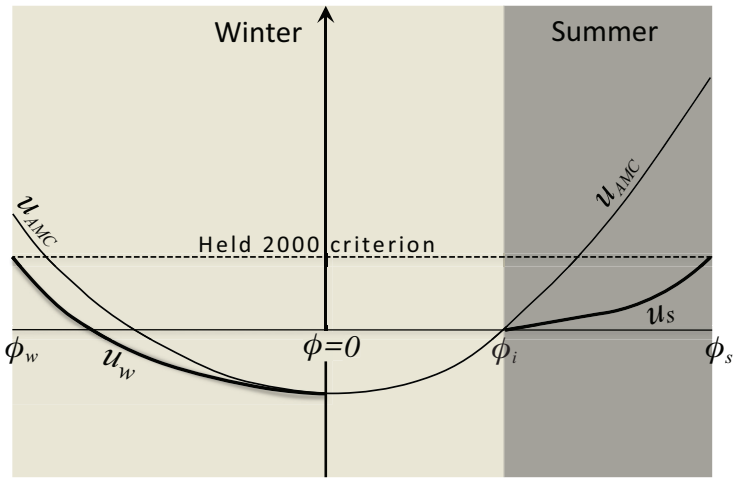

FIG. 1. Schematic for a scaling relation that distinguishes the winter from the summer HC. The thin solid line represents the angular momentum conserving zonal-wind profile (u_{AMC}), obtained under the assumption of u=0 at the ITCZ, ϕ_i. The dashed line indicates the Held (2000) criterion for baroclinic instability and hence the edge of the Hadley cell. The zonal wind in summer (u_s) deviates more from u_{AMC} compared to the zonal wind in winter (u_w), suggestive of larger Ro in winter, so that the HC edge in summer (ϕ_s) reaches higher latitudes than that in winter (ϕ_w).

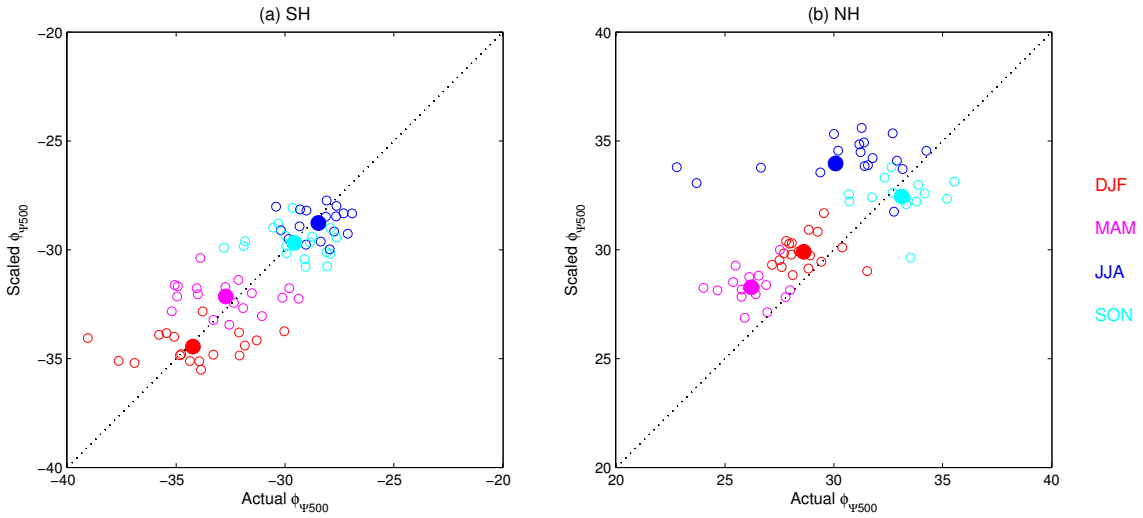

FIG. 2. The first 20 year mean of the HC edge vs its scaling for the (a) SH and (b) NH from 1pctto2x scenario for each season (DJF in red; MAM in pink; JJA in blue; SON in cyon). The ensemble-mean response is denoted by large filled circles.

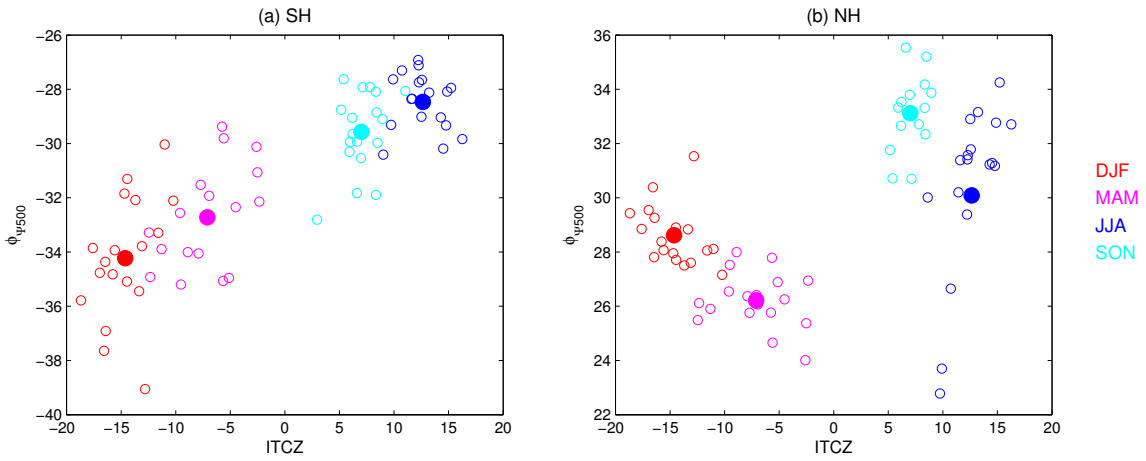

FIG. 3. The first 20 year mean of the ITCZ vs the HC edge for the (a) SH and (b) NH from 1pctto2x scenario for each season (DJF in red; MAM in pink; JJA in blue; SON in cyon). The ensemble-mean response is denoted by large filled circles.

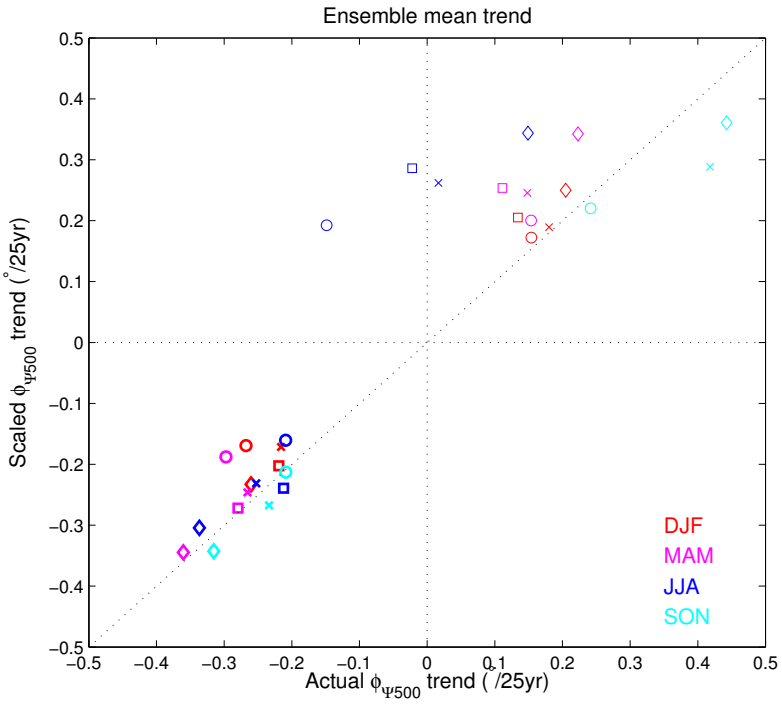

FIG. 4. The ensemble-mean trend of the HC edge vs its scaling for the SH in thick markers and for the NH in thin markers for each season (DJF in red; MAM in pink; JJA in blue; SON in cyon). 1pctto2x in circle, 1pctto4x in square, A1B in cross, and A2 in diamond.

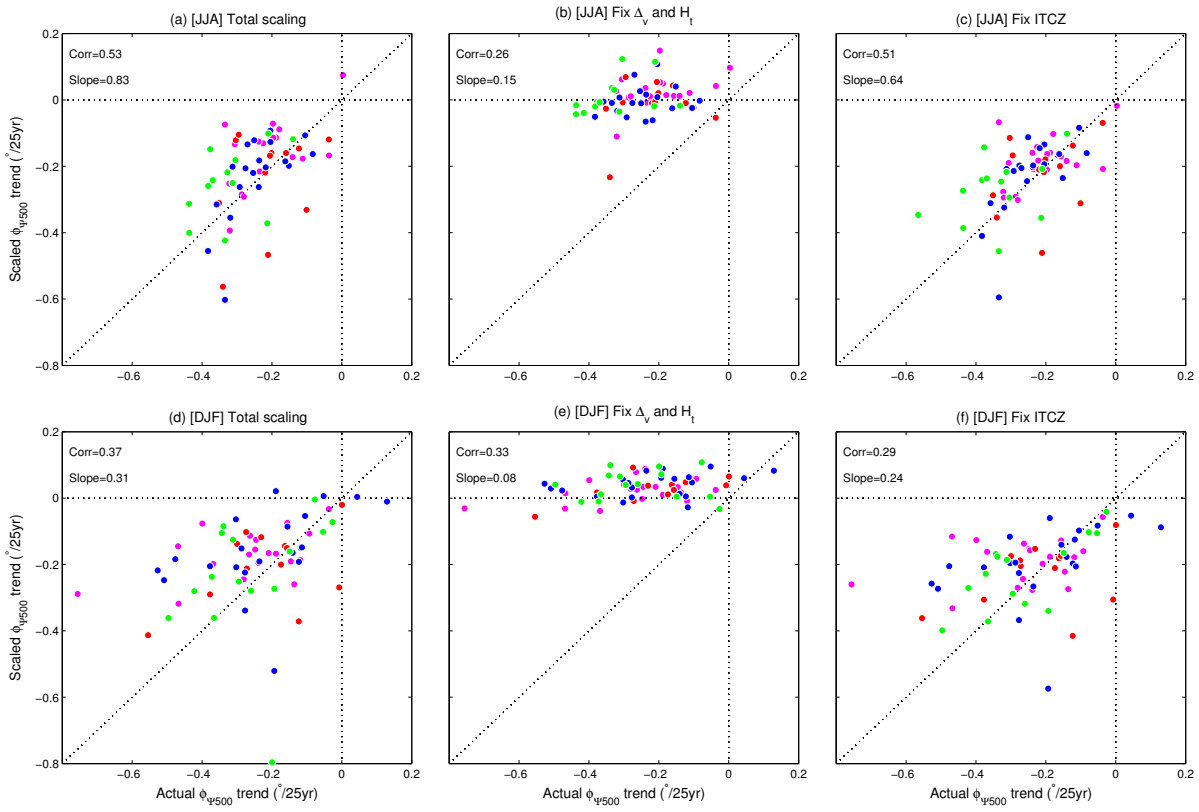

FIG. 5. The HC edge trend vs its scaling for the SH in (upper) JJA and (lower) DJF. The ordinates in the left panels denote the total scaling, those in the middle panels denote the scaling with Δ_v and H_t fixed to their first 20 year mean, and those in the right panels denote the scaling with the ITCZ latitude fixed to its first 20 year mean. 1pctto2x in pink, 1pctto4x in red, A1B in blue, and A2 in green. The correlation coefficient and slope between the actual HC edge and its scaling are given in the upper left corner of each panel.

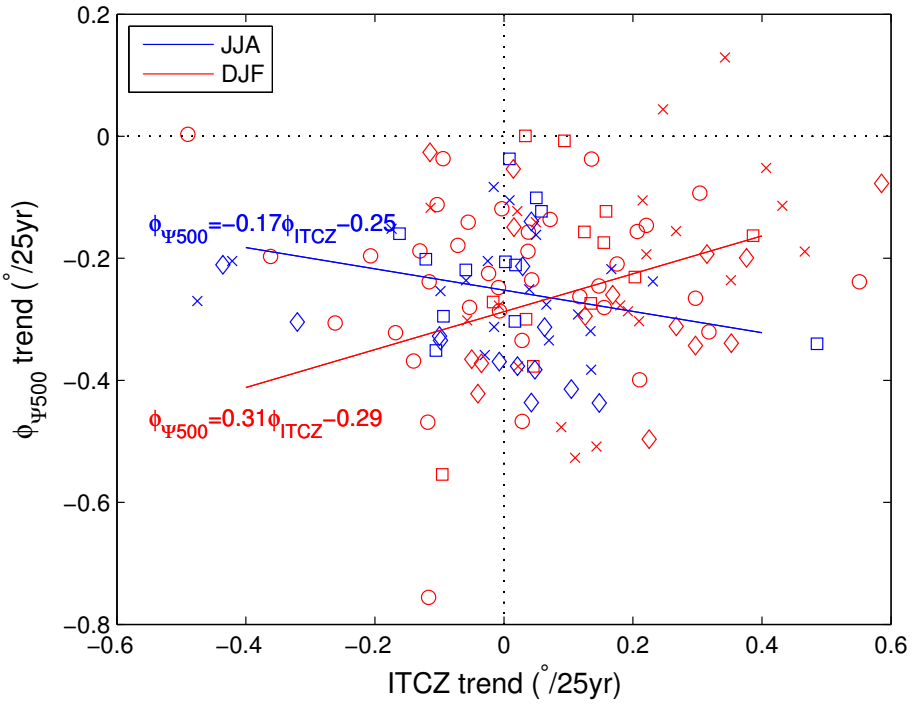

FIG. 6. The trend of the ITCZ vs that of the HC edge for the SH in JJA (blue) and DJF (red). 1pctto2x in circle, 1pctto4x in square, A1B in cross, and A2 in diamond.